



Photocatalytic H₂ evolution with a Cu₂WS₄ catalyst on a metal free D-π-A organic dye-sensitized TiO₂

Emre Aslan^a, Mehmet Kerem Gonce^b, Mesude Zeliha Yigit^c, Adem Sarilmaz^d, Elias Stathatos^e, Faruk Ozel^d, Mustafa Can^f, Imren Hatay Patir^{g,*}

^a Selcuk University, Department of Chemistry, 42030, Konya, Turkey

^b Selcuk University, Department of Nanotechnology and Advanced Materials, 42030, Konya, Turkey

^c Izmir Katip Celebi University, Department of Material Science and Engineering, Faculty of Engineering and Architecture, 35620, Izmir, Turkey

^d Karamanoglu Mehmetbey University, Department of Metallurgical and Materials Engineering, 70200, Karaman, Turkey

^e Nanotechnology and Advanced Materials Laboratory, Department of Electrical Engineering, Technological-Educational Institute of Western Greece, GR-26334 Patras, Greece

^f Izmir Katip Celebi University, Faculty of Engineering and Architecture, Department of Engineering Sciences, Cigli, 35620 Izmir, Turkey

^g Selcuk University, Department of Biotechnology, 42030, Konya, Turkey

ARTICLE INFO

Article history:

Received 14 January 2017

Received in revised form 28 March 2017

Accepted 29 March 2017

Available online 31 March 2017

Keywords:

Hydrogen evolution

Hot-injection

Cu₂WS₄ catalyst

Dye sensitization

ABSTRACT

A system comprising of a noble metal free Cu₂WS₄ catalyst and donor-π-bridge-acceptor metal-free organic dyes (MZ-341 and MZ-235) sensitized TiO₂ has been reported for the photocatalytic hydrogen production using triethanolamine (TEOA) as the sacrificial reagent under visible light irradiation. Cu₂WS₄ nanocubes were synthesized according to hot-injection reaction technique. The structural properties of the Cu₂WS₄ nanocubes were examined by microscopy (HR-TEM) and XRD techniques where the formation of nanocubes (rectangular and square cubes) with average edge length to be ranged from 100 to 500 nm and tetragonal phase (*I*-42m) was proved respectively. It was found that MZ-341 and MZ-235 dyes sensitized TiO₂ have been produced 661 μmol g⁻¹ h⁻¹ and 531 μmol g⁻¹ h⁻¹ hydrogen, respectively in TEOA solution at pH 9. When Cu₂WS₄ was used as a co-catalyst, hydrogen evolution by MZ-341 and MZ-235 sensitized TiO₂ have been slightly increased to 1406 μmol g⁻¹ h⁻¹ and 943 μmol g⁻¹ h⁻¹, respectively.

© 2017 Elsevier B.V. All rights reserved.

1. Introduction

Since the pioneer report on water splitting for hydrogen evolution over TiO₂ electrodes under UV irradiation by Honda and Fujishima a great deal of attention has been paid to photocatalytic hydrogen evolution from water using nanostructured semiconductors [1]. To date, a large number of TiO₂ based photocatalysts have been used for efficient hydrogen evolution via water splitting [2–7]. The drawbacks of the TiO₂ semiconductor is that it absorbs a small portion of the solar spectrum in the UV region due to its wide band gap of 3.2 eV, it shows fast rates of electron-hole recombination and finally requires a high over potential for water splitting reaction. Photocatalytic activity of TiO₂ can be extensively increased by (i) dye-sensitization of TiO₂ for visible light utilization [8–10], and (ii) co-attachment of an efficient hydrogen evolution catalysts such

as noble metal based catalysts especially Pt [11–13], or noble metal free catalysts [14].

In the case of dye sensitization of semiconductors, metal-free organic dyes have recently been aroused great interest due to their high molar extinction coefficients, availability of various ways to design donor-π-bridge-acceptor (D-π-A), low cost, and environmentally friendly nature. Particularly, xanthene dyes, D-π-A organic dyes and cation organic dyes have been used as effective dyes for the sensitization of semiconductors in the visible region of light [15–27].

Recently, D-π-A organic dyes displayed good photovoltaic performance and photocatalytic activity in dye sensitized solar cells (DSSC) applications [28] and dye-sensitized hydrogen evolution systems owing to their absorption properties and appropriate modulation of the intramolecular charge transfer character [15,16,23,27,29]. The most popular electron donor moieties of these dyes are triphenylamine, merocyanine, carbazole, phenothiazine, coumarin and their derivatives. The significance of hydrophilic and steric characteristics of triphenylamine-based dyes sensitized

* Corresponding author.

E-mail address: imrenhatay@gmail.com (I.H. Patir).

Pt/TiO₂ was investigated in H₂ evolution systems by Kang's group [30,31]. The influence of the number of anchoring groups on the triphenylamine-based dye sensitized TiO₂ for H₂ evolution was explored also by Park's group [32]. Moreover, Yang and Zheng's group were reported the investigation of triphenylamine based dyes (TPA) covalently functionalized graphene (G-TPA) and platinum nanoparticles modified G-TPA nanocomposites (Pt/GTPA) as a photocatalyst for H₂ production [33].

As mentioned above, the photocatalytic activity of TiO₂ semiconductors can be also increased by using co-catalysts, which are commonly based on noble metals (Pt, Ru, Rh, Pd, etc.) or their alloys due to their lowest over potential and larger work function for H₂ production. The research progress of co-catalysts containing non-noble metals is essentially desirable for practical applications because of the scarcity and cost of noble metals. Recently, a number of co-catalysts without noble metal such as inorganic Ni, Cu, Co, Mo, W based species are promising noble metal free co-catalysts in dye-sensitized semiconductor systems [27,34–36]. For instance, catalysts based on WS₂, MoS₂, MWS_x and MMoS_x (M = Co, Ni, Cu) have been investigated for the electrocatalytic and photocatalytic hydrogen evolution reactions [37–45]. Until now, the hydrogen evolution activity of Cu₂WS₄ catalyst has been rarely investigated. In particular, it has been electrocatalytically investigated by our group [41] and photocatalytically by other research groups [42,43]. However, there has been no report on the application of Cu₂WS₄ material as H₂ evolution catalyst in dye sensitized systems.

Herein, we report for first time on hydrogen evolution reaction by using a triphenylamine-based two organic dyes with D-π-A structure sensitized TiO₂ in the presence and absence of Cu₂WS₄ catalyst, which is synthesized by hot-injection method. The photoelectrocatalytic hydrogen evolution behavior of MZ-341 (4-[4-(diphenylamino)phenyl]-7-oxo-7Hbenzimidazo[2,1-a]benzo[de]isoquinoline-11-carboxylic acid) and MZ-235 (4-(4-{bis[4-(hexyloxy)phenyl]amino}phenyl)-7-oxo-7H-benzimidazo[2,1-a]benzo[de]isoquinoline-11-carboxylic acid) on the TiO₂ composite electrodes have been investigated by chronoamperometric measurements. The photocatalytic hydrogen evolution rate of MZ-341/TiO₂, MZ-341/TiO₂/Cu₂WS₄, MZ-235/TiO₂ and MZ-235/TiO₂/Cu₂WS₄ has been also compared with each other by using triethanolamine (TEOA) as the sacrificial electron donor under visible light irradiation. Furthermore, the possible photocatalytic hydrogen production mechanism and the role of Cu₂WS₄ catalyst are also discussed.

2. Experimental section

2.1. Synthesis of dyes

All solvents and reagents, unless otherwise stated, were of puriss quality and used as received. Bromohexane and Cul were purchased from Merck. [1,10-bi(diphenylphosphino) ferrocene]dichloropalladium(II), trimethylborate, n-butyllithium, dichloromethane, 1,2-dimethoxyethane (DME), 1,10-phenanthroline, toluene, 18-crown-6, acetone, tetrahydrofuran (THF) and triethanolamine (TEOA) were purchased from Sigma-Aldrich. P-bromoaniline and p-lodophenol were purchased from Riedel de Haen. KOH and K₂CO₃ were purchased from Alfa Aesar. The organic dyes synthesis procedures were described in our previous publication [46].

2.2. Synthesis of Cu₂WS₄

Previous published findings revealed that, hot injection synthesis is a new approach to synthesize Cu₂WS₄ to decrease the reaction time and required pressure. Herein, Cu₂WS₄ nanocubes

were synthesized using the previously published hot-injection reaction technique [41]. In this process, 1 mmol copper (II) Chloride hydrate and 0.5 mmol tungsten (IV) chloride were loaded into a 25 mL three-neck flask containing 10 mL of oleylamine (OLA) and heated to 180 °C under Ar flow. The color of the solution changed to black after the injection of a mixture of 2 mL OLA including 64 mg sulfur powder. Afterwards, the temperature of the solution was increased to 300 °C and kept for 30 min by stirring. After the reaction, the nanocubes were centrifuged at 4000 rpm for 5 min with 35 mL toluene and 5 mL ethanol mixture. Finally, the crystals were washed with ethanol, dried and stored under vacuum.

2.3. Instrumentation

The crystal structures and microstructures of the as-prepared nanocubes were characterized by Bruker Advance D8 X-ray diffractometer (XRD) (Cu α source with 1.5406 wavelengths) and transmission electron microscope (JEOL JEM-2100F). Optical and electrochemical properties of materials were investigated by Shimadzu UV-1800 spectrometer and CH-760D potentiostat, respectively. Solar Light XPS-300™ was used as the light source in the photocatalytic and photoelectrochemical hydrogen evolution reaction setup. Produced hydrogen gas was analyzed with a gas chromatograph (GC; Shimadzu GC-2100 Plus). GC was calibrated for standard H₂ concentration sample in the N₂ from 0.1% to 5%.

2.4. Dye sensitization process

Prior any use of powder TiO₂ (Degussa P25) it was calcined at 450 °C for 45 min. The calcination of TiO₂ was applied to remove any organic contaminants and adsorbed water. It is very important before binding between TiO₂ and dye molecules the surface of the semiconductor to be free from any contaminant could influence the adsorption of the dyes. Then the prepared dye solution (10⁻⁵ M in THF) and previously calcined TiO₂ were mixed and stirred overnight under dark conditions. After stirring, sensitized TiO₂ was filtered and rinsed in triplicate with THF and ethanol, respectively. This sensitization process was done individually for each dye for the photocatalytic hydrogen evolution reaction. Preparations of dye sensitized photoelectrodes for the photoelectrochemical hydrogen evolution commercial TiO₂ coated FTO electrodes (Dyesol MS 001630) were used and these electrodes were also calcined at 450 °C for 45 min prior the sensitization process. Calcined electrodes were kept in the dye solution (10⁻⁵ M in THF) in the dark conditions overnight. After sensitization process, sensitized TiO₂ electrodes were rinsed in triplicate with THF and ethanol, respectively.

2.5. Photocatalytic hydrogen evolution

Photocatalytic hydrogen evolution reaction was performed under oxygen-free media and visible light illumination ($\lambda \geq 420$ nm, Solar Light XPS-300™). TEOA solution was used as a sacrificial electron donor. Hybrid photocatalyst (dye/TiO₂), hydrogen evolution catalyst (Cu₂WS₄ or Pt) and electron donor solution (TEOA) were added in the photo-reaction cell (total volume 135 mL) in the glovebox under N₂ atmosphere, and then this photo-reaction cell was sealed with rubber septa. After this preparation, photo-reaction cell was put out from glove-box system and then this mixture was suspended in 20 mL TEOA under ultrasonic treatment. After all these processes, photocatalytic hydrogen evolution reaction was begun under visible light irradiation and continuous stirring. Finally, the produced hydrogen was calculated after periodical sampling from materials mixture in the headspace.

2.6. Photoelectrochemical measurements

Photoelectrochemical measurements were carried out under N_2 flow, stirring condition and visible light illumination ($\lambda \geq 420$ nm). The combination of aqueous TEOA (0.3 M) and Na_2SO_4 (0.1 M) solutions at pH 9 was used as the electrolyte for the same condition of photocatalytic hydrogen evolution. Three-electrode cell using a potentiostat (CHI-760D) was used for the investigation of their photoelectrochemical properties. The prepared dye sensitized photoelectrodes were used as the working electrodes. Pt wire and Ag/AgCl electrodes were used as counter and reference electrode, respectively. Linear sweep voltammograms were recorded at a scan rate of 5 mVs^{-1} aqueous electrolyte solutions while the scan region was from -0.6 V to 0.6 V . Chronoamperometric measurements were performed for 350 s where the light was kept on for 50 s and off for 50 s.

3. Results and discussions

3.1. Structural characterization

The FT-IR spectra of dyes and dyes' sensitized TiO_2 electrodes are shown in Fig. S1. Hydroxyl bonds (O–H) of MZ-341 and MZ-235 dyes were observed in 3359 and 3389 cm^{-1} , respectively. Also carbonyl bonds (COOH) of MZ-341 and MZ-235 dyes are observed in 1667 and 1703 cm^{-1} , respectively. However, it was found that those peaks (carbonyl and hydroxyl bonds) were disappeared in the case of dyes sensitized TiO_2 films because of their chemical adsorption on TiO_2 . According to FT-IR results, it is obvious that organic molecules were linked chemically to TiO_2 .

The morphology of the $I\text{-Cu}_2WS_4$ nanocubes was examined by TEM and is illustrated in Fig. 1. As can be clearly seen from Fig. 1(a), the nanocubes are formed as rectangular and square cubes with the average edge length to be ranged from 100 to 500 nm. To further confirm the structure of the nanocubes, High Resolution-TEM analysis has been carried out. As can be clearly seen from Fig. 1b, clear lattice fringes with an average interplanar distance of 0.52 nm, corresponding to (002) planes of body centered tetragonal phase Cu_2WS_4 . The SAED pattern of a randomly chosen region of the nanocubes (Fig. 1c) indicates that the nanocubes have a single crystalline in nature. Moreover the sharp spots on the pattern indicate that the nanocubes are well crystallized. Consequently, all of the obtained results are compatible with XRD results.

Fig. 2a illustrates the X-ray diffraction (XRD) pattern of the prepared nanocubes. All the diffraction peaks of the synthesized

nanocubes can be readily indexed to the body centered tetragonal phase ($I\text{-}42m$) of Cu_2WS_4 (JCPDS no. 01-074-3742) with effective crystallization and lack the presence of any impurity [47]. No evidence of other phases can be found in the XRD pattern. Additionally, the inset of Fig. 2a shows the size distribution of the nanocubes determined by T-SAXS analysis and confirms the TEM results. In this study, we used TiO_2 (Degussa P25), which is a mixture of anatase and rutile in 8:2 ratio. Finally, X-ray diffraction (XRD) patterns of as received and annealed TiO_2 particles appear in Fig. 2b and c. The rate of anatase:rutile crystal phases in TiO_2 crystal was turned to 82:18 and 72:28 for the as-received and after calcination samples, respectively.

Moreover, X-ray photoelectron spectrum (XPS) of the Cu_2WS_4 catalyst has been performed before and after the photocatalytic reaction (Fig. S2). The survey X-ray photoelectron spectra reveal that the as-synthesized product is composed of Cu, W and S elements (Fig. S2a), which are in good agreement with the known values of the Cu_2WS_4 structures. However, after the photocatalytic reaction, the sample (2p orbital of S) showed only one peak (Fig. S2d), due to the hydrogenation of Cu_2WS_4 nanostructures, while the Cu_2WS_4 sample shows standard 2p S peaks (Fig. S2c). These results confirming that parts of sulfur in Cu_2WS_4 structure were hydrogenated during photocatalytic reaction [48].

3.2. Optical, electrochemical and photoelectrochemical properties of materials

Dyes exposed an absorption peak in close proximity to each other, about 439–441 nm for MZ-341 and 463–465 nm for MZ-235 as shown in Fig. 3(a). These peaks arise from $\pi\text{-}\pi^*$ transition, which may be ascribed to the HOMO-LUMO transition or intermolecular transfer of charges between the donor and the acceptor. Intermolecular charge transfer plays a vital role in dye-sensitized photocatalysis because the light is being collecting around the transition bands. Due to the addition of more electron donating groups on dye the spectrum was red shifted about 20 nm [46]. Oxidation potential is reduced by the addition of extra electron donating groups (like hexyloxy groups in our study) on the triphenylamine donor and resulted an increased HOMO level value of the MZ-235 dye. Absorption peaks of dye sensitized TiO_2 particles were monitored in 330 nm as shown in Fig. 3(b) and these were in the same condition of those used in photocatalytic hydrogen evolution (TEOA at pH=9). It was found that the absorption of MZ-341 dye on TiO_2 was higher than MZ-235 on TiO_2 [46]. Dyes having higher molar extinction coefficients may absorb more light and generate more

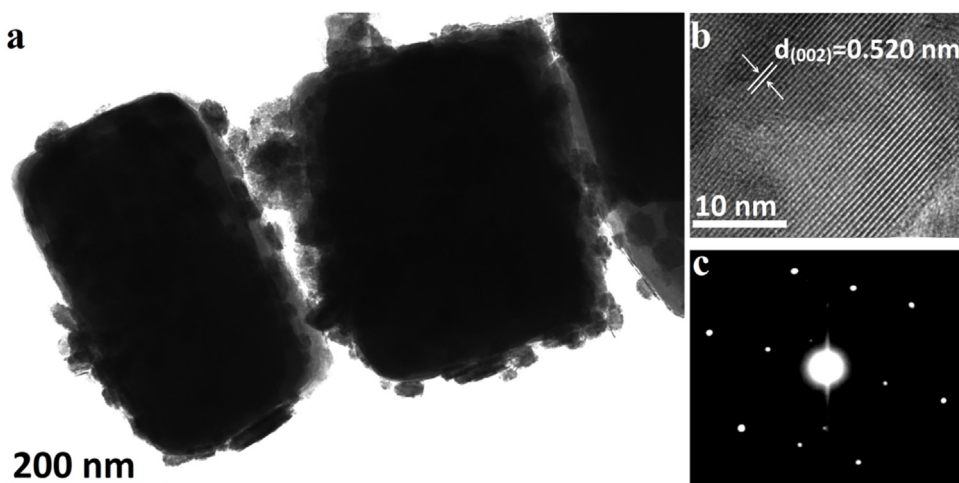


Fig. 1. TEM-HRTEM images and SAED pattern of the $I\text{-Cu}_2WS_4$ nanocubes.

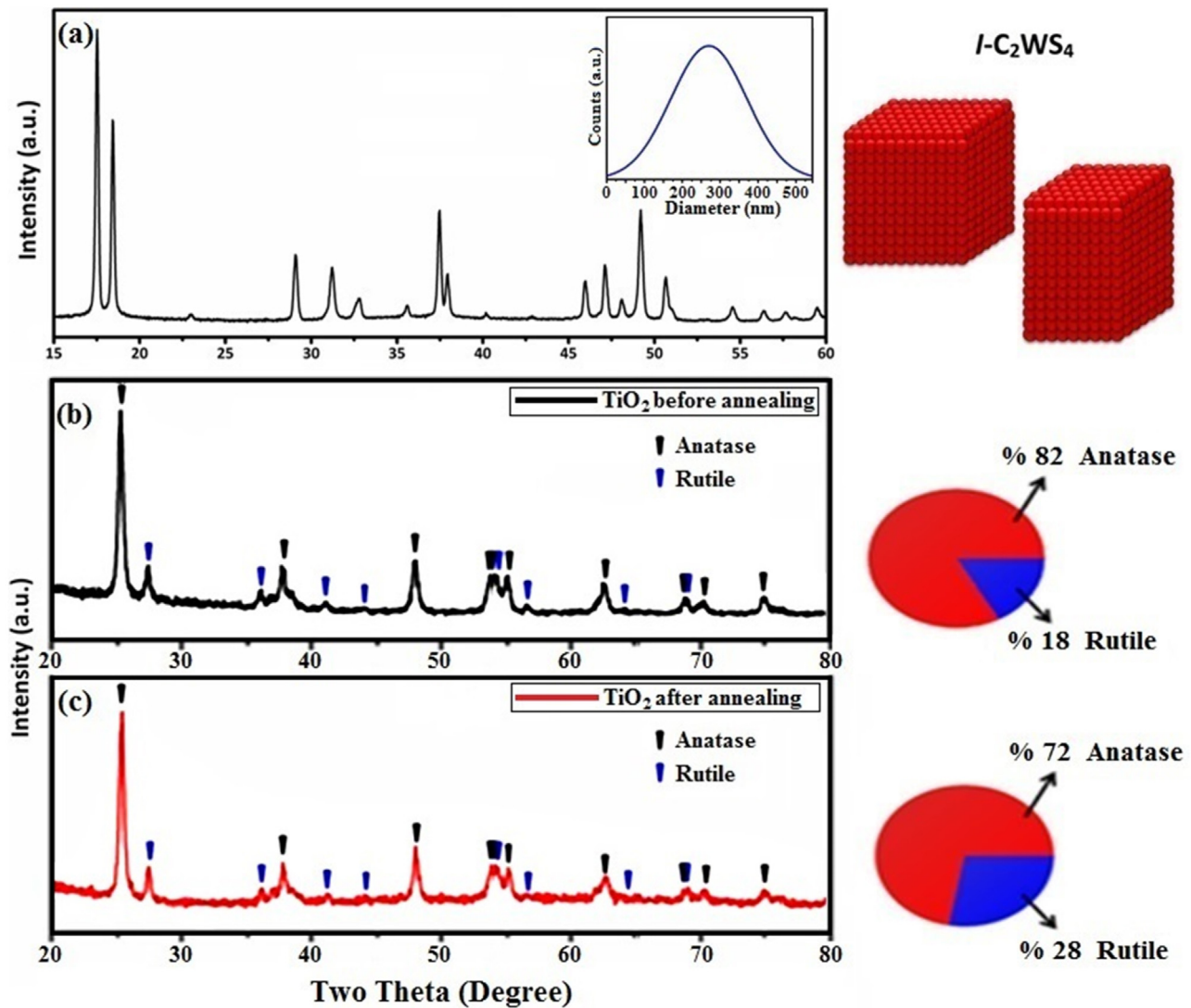


Fig. 2. X-ray diffraction patterns for $I\text{-Cu}_2\text{WS}_4$ nanocubes (inset: T-SAXS analysis of Cu_2WS_4) (a) and as-received (b) and after calcination (c) TiO_2 particles, [Cu K α radiation ($\lambda = 1.54\text{\AA}$)].

electrons under the same conditions [32,46]. In addition, dyes on the TiO_2 were calculated from absorption and elemental analysis as shown in SIS-2. Although the absorption of both dyes on TiO_2 is different, the amount of each dye on the film was quite similar. This result was concluded after dyes' extraction from the films when they were exposed in dilute NaOH. However, different dye loadings were also used for P25 sensitization in order to find the optimum concentration for hydrogen production. We tried different concentrations for both dyes at starting solutions. Namely we tried concentrations in the range of $10^{-3}\text{--}10^{-5}$ M where no worth mentioned differentiations in measured photocurrents were recorded under exposure to light.

Optical properties of Cu_2WS_4 nanocubes were investigated by UV-vis spectrophotometer and the results are shown in Fig. 3c. It shows that the nanocubes have a strong absorption at higher energies, which present high optical absorption from the ultra-violet region to the near infrared spectrum. Moreover the optic band gap of the nanocubes was estimated as 1.80 eV by the related curve $(\alpha h)^2$ versus photon energy by using the intersection of the extrapolated linear portion of the curve, which proves itself to be a promising candidate in future fabrication of cost-effective, high efficiency energy conversion applications.

The electrochemical properties of the dyes and Cu_2WS_4 were investigated by the cyclic voltammetry in the tetrabutylammonium hexafluorophosphate (Bu_4NPF_6) solution in acetonitrile. Glassy-carbon, Ag/AgCl and platinum wire were used as the working electrode, reference electrode and counter electrode, respectively. The oxidation potentials of MZ- 235 and MZ-341 were found at 0.977 V and 1.087 V (vs. NHE), while HOMO levels were found 5.18 and 5.30 eV, respectively. The reduction potentials and LUMO levels were found according to our previous studies at -0.933 V and 3.27 eV for MZ-341 and at -0.936 and 3.24 eV for MZ- 235 [46]. Electrochemical band levels (conduction band and valance band) of Cu_2WS_4 were calculated from cyclic voltammogram appear in Fig. 3d. Conduction band of Cu_2WS_4 was found at -0.163 V vs. NHE. High current at about +1.6 V could be pointed out as valence band level. The calculated electronic bandgap (~ 1.44 eV) have been found in close proximity to that obtained from optical measurements.

The aforementioned two dyes (MZ-341 and MZ-235) were previously examined in dye sensitized solar cell applications [46]. TiO_2 coated FTO, Ag/AgCl and Pt electrodes were used as the working, reference and, counter electrodes, respectively. Working electrode acts as a photoanode because n-type semiconductors like TiO_2 are

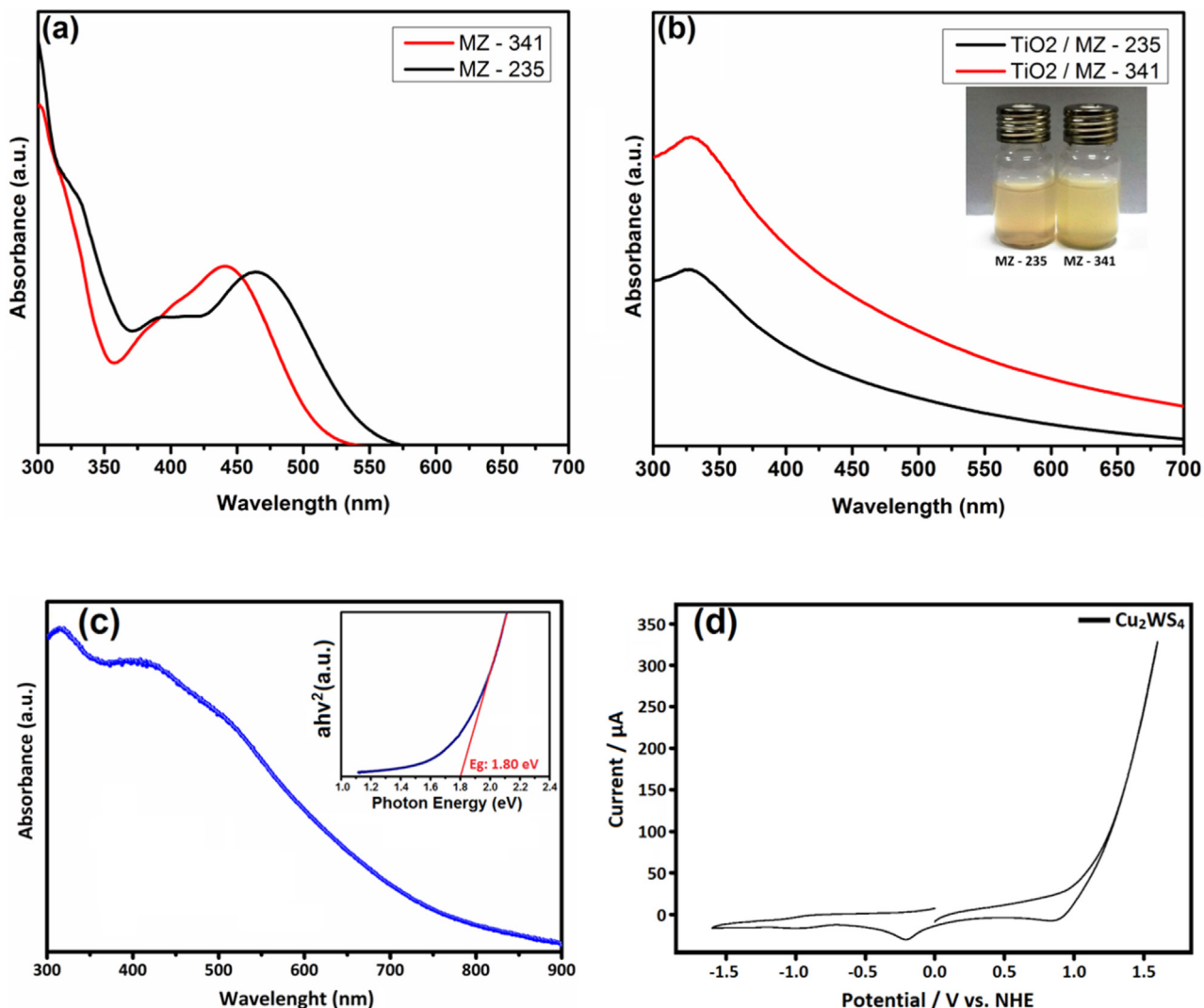


Fig. 3. (a) UV-vis spectra of dyes in THF, (b) UV-vis spectra of dye/TiO₂ in TEOA and (c) UV-vis spectrum of Cu₂WS₄. The inset shows the calculated band gap of Cu₂WS₄, Tauc Plot. (d) Cyclic voltammogram of Cu₂WS₄ using 0.1 M Bu₄NPF₆ in acetonitrile (Scan rate: 100 mV s⁻¹).

generally employed in fabrication of photoanodes [49]. In general, hydrogen is produced on the Pt cathode because the photogenerated electrons are transferred from photoanode to cathode.

In this study, photoelectrochemical experiments were performed in aqueous TEOA (0.3 M) and Na₂SO₄ (0.1 M) solution at pH 9 acting as electron donor and electrolyte respectively, under visible light source ($\lambda \geq 420$ nm) and N₂ flow under stirring. Linear sweep voltammetry (LSV) and chronoamperometric measurements were carried out in the absence and presence of dyes on TiO₂ electrodes. LSV experiments have been examined from +0.6 V to -0.6 V, and very stable results were obtained for all these potentials (see SI, Fig. S4). Afterwards, chronoamperometric measurements were performed for 350 s with 50 s the light was off while 50 s the light was on. Fig. 4a and b show photoelectrochemical response of the FTO electrodes covered with TiO₂ under visible light irradiation in the absence and presence of dye sensitization. The photocurrent response for the dye/TiO₂ electrodes were instant, stable and consistent during repeated on/off cycles under illumination. The blank experiment using the bare FTO electrode did not produce photocurrent under the same irradiation conditions. However, TiO₂ coated FTO electrode created very weak photocurrent under the same conditions while this photocurrent value was in good agreement with literature [50]. The photocurrent density

reached 610 $\mu\text{A cm}^{-2}$ and 110 $\mu\text{A cm}^{-2}$ for the MZ-341 and MZ-235 sensitized TiO₂ electrodes, respectively. These results have shown that the photoelectrochemical activity of MZ-341 was higher than MZ-235 as shown in current density vs. time graphs in Fig. 4a. The current density differences of dye sensitized TiO₂ electrodes were in accordance with absorption of dyes (Fig. 4b) and photocatalytic hydrogen experiments.

3.3. Photocatalytic performances of dye-sensitized TiO₂ with Cu₂WS₄ co-catalyst

There are a few reports on dye sensitized photocatalytic hydrogen production using triphenylamine-based dyes [33,34]. Most of them use Pt as the co-catalyst with the dye sensitized TiO₂ [31,51]. In addition, covalently functionalized graphene with the same structural dye in the photocatalytic and photoelectrochemical hydrogen evolution was investigated by Yang and Zheng's group. The amount of produced hydrogen is very low which could be due to the absence of photocatalyst, like TiO₂ [33]. Photocatalytic hydrogen evolution experiments were carried out in aqueous TEOA solution (0.33 M) used as the sacrificial electron donor under visible light and continuous stirring conditions [52,53]. First of all, evolution of hydrogen was performed at different pH values ranged

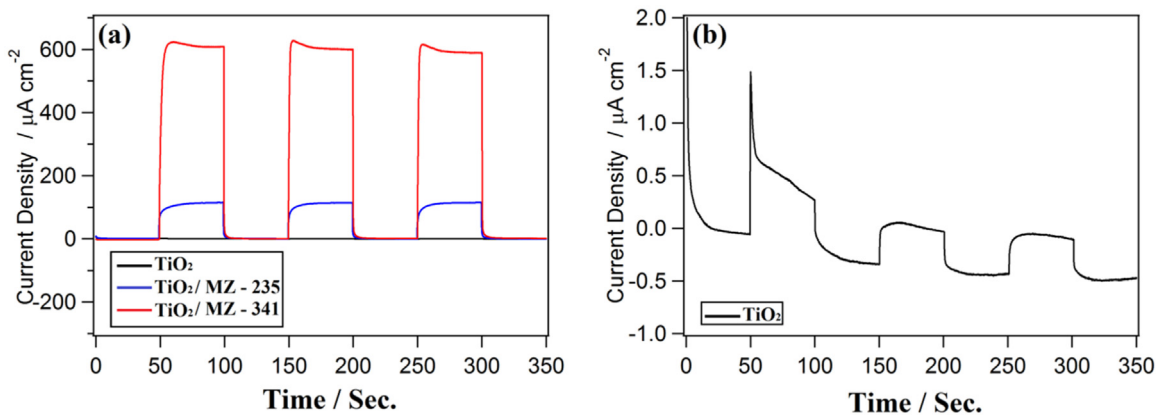


Fig. 4. Comparison of the photoelectrochemical response of (a) $\text{TiO}_2/\text{MZ}-341$ and $\text{TiO}_2/\text{MZ}-235$ with (b) only TiO_2 for HER (aqueous solution of 0.33 M TEOA and 0.1 M Na_2SO_4 at pH = 9 as the support electrolyte).

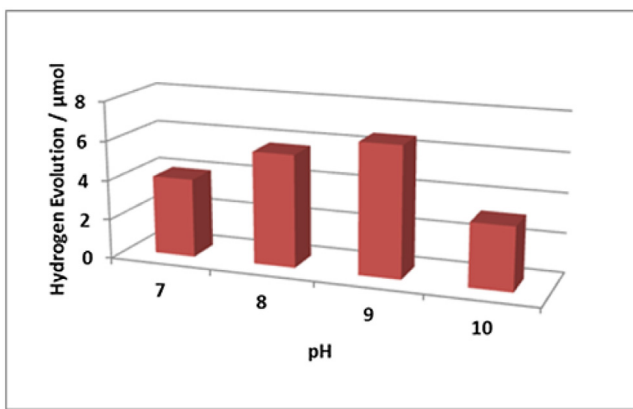


Fig. 5. Dependency of pH for the hydrogen evolution reaction in aqueous TEOA solution (0.3 M).

from 7 to 10 while pH 9 was finally the optimal value of pH for hydrogen evolution reaction in our system (Fig. 5). This pH value is in accordance with our previous published papers [54–56]. In addition, these results are compatible with the previous hydrogen production with triphenylamine-based dyes in TEOA solution [32].

Fig. 6 shows the time-profiled hydrogen evolution under visible light irradiation to dye/ $\text{TiO}_2/\text{Cu}_2\text{WS}_4$ suspensions in the presence of TEOA. The evolved hydrogen amount is normalized to the mass of dye sensitized TiO_2 . The HER rate of $\text{MZ}-341/\text{TiO}_2$, $\text{MZ}-341/\text{TiO}_2/\text{Cu}_2\text{WS}_4$, $\text{MZ}-235/\text{TiO}_2$ and $\text{MZ}-235/\text{TiO}_2/\text{Cu}_2\text{WS}_4$ was found to be $661 \mu\text{mol g}^{-1} \text{h}^{-1}$, $1406 \mu\text{mol g}^{-1} \text{h}^{-1}$, $531 \mu\text{mol g}^{-1} \text{h}^{-1}$ and $943 \mu\text{mol g}^{-1} \text{h}^{-1}$, respectively. After 8 h of visible light irradiation, the amount of evolved hydrogen with $\text{MZ}-341/\text{TiO}_2$, $\text{MZ}-341/\text{TiO}_2/\text{Cu}_2\text{WS}_4$, $\text{MZ}-235/\text{TiO}_2$ and $\text{MZ}-235/\text{TiO}_2/\text{Cu}_2\text{WS}_4$ was $5505 \mu\text{mol g}^{-1}$, $6340 \mu\text{mol g}^{-1}$, $4240 \mu\text{mol g}^{-1}$ and $4650 \mu\text{mol g}^{-1}$, respectively. The control experiments were performed in this system by using solely TiO_2 , or Cu_2WS_4 or finally $\text{TiO}_2/\text{Cu}_2\text{WS}_4$ in the absence of dyes under visible light irradiation. It was found that there was no hydrogen gas detection in the absence of dyes. In addition, the catalytic HER activity of dye/ TiO_2 composites has been compared to that of Pt particles and using xanthane dye eosin-y under the same conditions (see SI, Fig. S5 for details). The produced hydrogen from TiO_2 sensitized with $\text{MZ}-341$ and $\text{MZ}-235$ were found to be lower than in the presence of Cu_2WS_4 . Hydrogen production was linear with irradiation time with the following order of activity: $\text{MZ}-341/\text{TiO}_2 > \text{MZ}-235/\text{TiO}_2$. When Cu_2WS_4 was added to the reaction media, the produced hydrogen amount was increased in comparison with the case of Cu_2WS_4 absence. The activity of

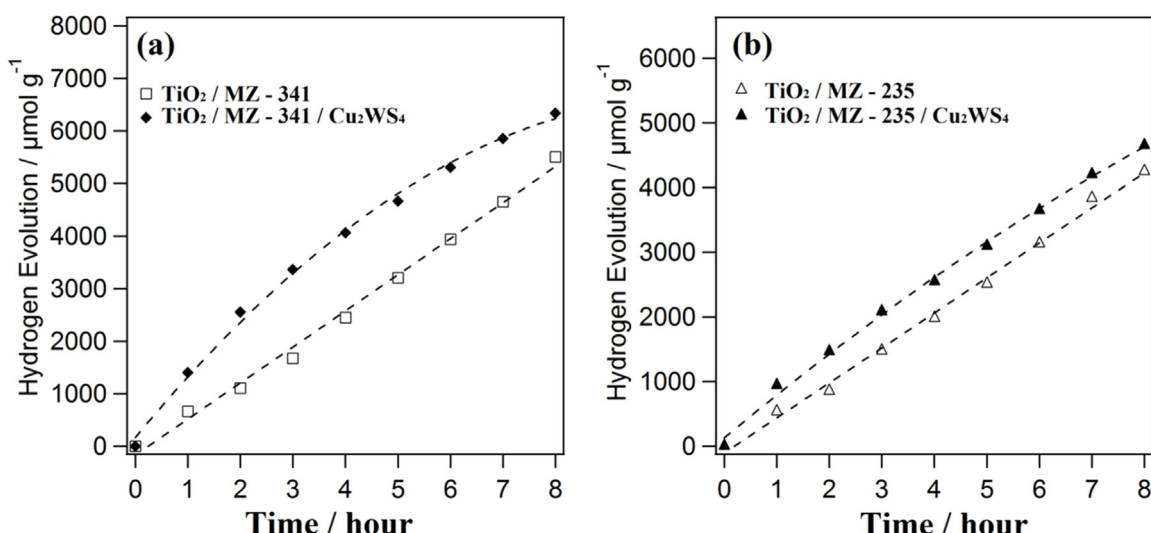


Fig. 6. Comparison of the photocatalytic activity of (a) $\text{TiO}_2/\text{MZ}-341$, $\text{TiO}_2/\text{MZ}-341/\text{Cu}_2\text{WS}_4$ and (b) $\text{TiO}_2/\text{MZ}-235$, $\text{TiO}_2/\text{MZ}-235/\text{Cu}_2\text{WS}_4$ for HER (10 mg TiO_2 /dye and/or 10 mg Cu_2WS_4 presence of TEOA (0.33 M) in 20 mL H_2O at pH = 9).

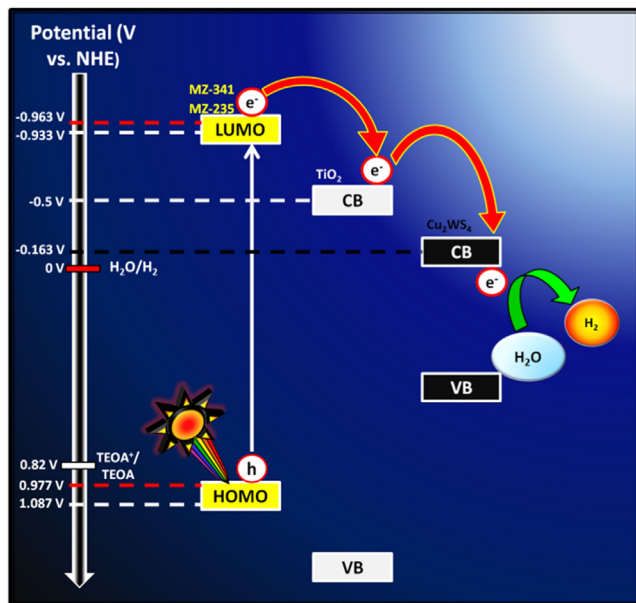


Fig. 7. Schematic of proposed photocatalytic hydrogen evolution reaction mechanism.

MZ-341 on the TiO_2 is higher than that of MZ-235. This difference of activity between MZ-341 and MZ-235 may be attributed to three factors; (i) MZ-341 exhibits higher absorption for sensitized TiO_2 film compared to that measured for MZ-235 as it can be seen in Fig. 3(b); (ii) the current densities of dyes in cyclic voltammograms showed that the current density of MZ-341 is larger than that of MZ-235 [46]; (iii) the photocurrent density differences of dyes on TiO_2 photoelectrodes can be also imputed (Fig. 4a).

Herein, the two triphenylamine-based organic dyes, MZ-341 and MZ-235, showed high efficient performances in visible light-driven hydrogen evolution. The difference between the HER rate of MZ-341 and MZ-235 could be ascribed to the light absorption ability MZ-235 and MZ-341 on TiO_2 (Fig. 3b). The proposed mechanism of hydrogen evolution reaction is shown in Fig. 7. According to this mechanism, visible light is absorbed by dyes (MZ-341 and MZ-235) therefore electrons are excited from HOMO to LUMO levels of the dyes. The photo-excited electrons can be transferred to the TiO_2 because of the fact that the conduction band level of TiO_2 is lower than LUMO levels of both dyes [46,57]. Finally, water is reduced by photo-excited electrons on the conduction band of TiO_2 and then holes in the dyes refilled by electrons from TEOA (reduction potential of $\text{TEOA}^+/\text{TEOA}$ is 0.82 V vs. NHE) to continue the hydrogen evolution reaction. Absorption property of the dyes is a fundamental factor determining the sensitization efficiency of the dye/ TiO_2 system [32,46]. When Cu_2WS_4 is added to the reaction media, mechanism is complicated than that of only dye/ TiO_2 system. Cu_2WS_4 plays a role to the hydrogen evolution as co-catalyst in this system instead of Pt. Electron transfer from dye to water is carried out gradually when Cu_2WS_4 and dye/ TiO_2 found at the same time in the reaction media. Electron transfer is begun from excited dye to the conduction band of TiO_2 , and then these electrons transferred to the conduction band of Cu_2WS_4 . Water is reduced by excited electrons on the Cu_2WS_4 . Finally, holes in the dyes refilled by TEOA. This mechanism is thermodynamically favourable. Light is absorbed by dyes (E_{ox} = oxidation potentials were found at 0.977 V and 1.087 V vs. NHE to form the excited state -0.933 V and -0.963 V for MZ-235 and MZ-341, respectively.) [46]. Electrons liberated from excited states of dyes are transferred to the CB of the Cu_2WS_4 . This reaction proceeds readily because the CB levels

of the Cu_2WS_4 nanocubes are more negative than the reduction potential of H^+/H_2 (0 V vs. NHE) [58].

4. Conclusions

Two triphenylamine and p-bridge, benzimidazole based organic dyes (MZ-341 and MZ-235) with or without additional electron donating hexyloxy groups have been used as sensitizer in the hydrogen evolution reaction. The hydrogen evolution activity of organic dyes sensitized TiO_2 has been investigated in the presence and absence of Cu_2WS_4 catalyst. The hydrogen evolution activity of MZ-341/ TiO_2 composite is higher than that of MZ-235/ TiO_2 , which could be mainly ascribed to the light absorption ability difference of the dyes. Moreover, the addition of Cu_2WS_4 catalyst results in barely increased catalytic activity, when compared to a non-catalysed reaction. This work shows the new way to study for solar energy conversion with dye- TiO_2 -metal sulfide catalysts, which have cheap processing, stability, simplicity and high yield of hydrogen evolution.

Acknowledgment

The authors would like to thank TUBITAK (The Scientific and Technological Research Council of Turkey) (215M309) for supporting this work and also Selcuk and Karamanoglu Mehmetbey University for Scientific Research Foundation. We also gratefully acknowledge the research support of Turkish Academy of Sciences via a TUBA-GEBIP fellowship. This paper is the part of Ph.D thesis prepared by Emre Aslan, which supported also by Selcuk University Scientific Research Projects (BAP). Dr. M. Can gratefully acknowledge the supports from of Izmir Katip Celebi University Grants Commission (Project Number: 2013-2-FMBP-17).

Appendix A. Supplementary data

Supplementary data associated with this article can be found, in the online version, at <http://dx.doi.org/10.1016/j.apcatb.2017.03.073>.

References

- [1] A. Fujishima, K. Honda, Nature 238 (1972) 37–38.
- [2] W.D.K. Clark, N. Sutin, J. Am. Chem. Soc. 99 (1977) 4676–4682.
- [3] M.T. Spitzler, M.J. Calvin, J. Chem. Phys. 66 (1977) 4294–4305.
- [4] A. Hammett, M.P. Dare-Edwards, R.D. Wright, K.R. Seddon, J.B. Goodenough, J. Phys. Chem. 83 (1979) 3280–3290.
- [5] M.P. Dare-Edwards, J.B. Goodenough, A. Hammett, K.R. Seddon, R.D. Wright, Faraday Discuss. Chem. Soc. 70 (1980) 285–298.
- [6] K. Zhang, Q. Liu, H. Wang, R. Zhang, C. Wu, J.R. Gong, Small 9 (2013) 2452–2459.
- [7] J. Li, G.R. Xu, B. Zhang, J.R. Gong, Appl. Catal. B 115 (2012) 201–208.
- [8] M. Watanabe, H. Hagiwara, A. Iribe, Y. Ogata, K. Shioiri, A. Staykov, S. Ida, K. Tanaka, T. Ishihara, J. Mater. Chem. A 2 (2014) 12952–12961.
- [9] J. Lee, J. Kwak, K.C. Ko, J.H. Park, J.H. Ko, N. Park, E. Kim, D.H. Ryu, T.K. Ahn, J.Y. Lee, S.U. Son, Chem. Commun. 48 (2012) 11431–11433.
- [10] W.J. Youngblood, S.H.A. Lee, K. Maeda, T.E. Mallouk, Acc. Chem. Res. 42 (2009) 1966–1973.
- [11] S.H. Lee, Y. Park, K.R. Wee, H.J. Son, D.W. Cho, C. Pac, W. Choi, S.O. Kang, Org. Lett. 12 (2010) 460–463.
- [12] E.A. Malinka, G.L. Kamalov, S.V. Vodzinskii, V.I. Melnik, Z.I. Zhilina, J. Photochem. Photobiol. A 90 (1995) 153–158.
- [13] E. Bae, W. Choi, J. Park, H.S. Shin, S.B. Kim, J.S. Lee, J. Phys. Chem. B 108 (2004) 14093–14101.
- [14] X.X. Zou, Y. Zhang, Chem. Soc. Rev. 44 (2015) 5148–5180.
- [15] R. Abe, K. Shinmei, N. Koumura, K. Hara, B. Ohtani, J. Am. Chem. Soc. 135 (2013) 16872–16884.
- [16] A. Tiwari, I. Mondal, U. Pal, RSC Adv. 5 (2015) 31415–31421.
- [17] C. Kong, S.X. Min, G.X. Lu, ACS Catal. 4 (2014) 2763–2769.
- [18] K.L.V. Joseph, J. Lim, A. Anthonyam, H.I. Kim, W. Choi, J.K. Kim, J. Mater. Chem. A 3 (2015) 232–239.
- [19] D. Duonghong, E. Borgarello, M. Gratzel, J. Am. Chem. Soc. 103 (1981) 4685–4690.
- [20] V.H. Houlding, M. Grätzel, J. Am. Chem. Soc. 105 (1983) 5695–5696.

[21] K. Gurunathan, P. Maruthamuthu, M. Sastri, *Int. J. Hydrogen Energy* 22 (1997) 57–62.

[22] A.A. Nada, H.A. Hamed, M.H. Barakat, N.R. Mohamed, T.N. Veziroglu, *Int. J. Hydrogen Energy* 33 (2008) 3264–3269.

[23] M. Latorre-Sánchez, C. Lavorato, M. Puche, V. Fornes, R. Molinari, H. Garcia, *Chem. Eur. J.* 18 (2012) 16774–16783.

[24] A. Kumari, I. Mondal, U. Pal, *New J. Chem.* 39 (2015) 713–720.

[25] H. Hagiwara, M. Nagatomo, S. Ida, T. Ishihara, *Energy Proc.* 22 (2012) 53–60.

[26] L. Zhang, W.Z. Wang, S.M. Sun, Y.Y. Sun, E. Gao, J. Xu, *Appl. Catal. B* 132 (2013) 315–320.

[27] X. Zhang, T. Peng, S. Song, *J. Mater. Chem. A* 4 (2016) 2365–2402.

[28] Y. Wu, W. Zhu, *Chem. Soc. Rev.* 42 (2013) 2039–2058.

[29] R. Abe, K. Sayama, H. Sugihara, *J. Sol. Energy Eng.* 127 (2005) 413–416.

[30] S.H. Lee, Y. Park, K.R. Wee, H.J. Son, D.W. Cho, C. Pac, W. Choi, S.O. Kang, *Org. Lett.* 12 (2010) 460–463.

[31] W.S. Han, K.R. Wee, H.Y. Kim, C. Pac, Y. Nabeta, D. Yamamoto, T. Shimada, H. Inoue, H. Choi, K. Cho, S.O. Kang, *Chem. Eur. J.* 18 (2012) 15368–15381.

[32] S.K. Choi, H.S. Yang, J.H. Kim, H. Park, *Appl. Catal. B* 121 (2012) 206–213.

[33] Z. Li, Y.J. Chen, Y.K. Du, X.M. Wang, P. Yang, J.W. Zheng, *Int. J. Hydrogen Energy* 37 (2012) 4880–4888.

[34] J.R. Ran, J. Zhang, J.G. Yu, M. Jaroniec, S.Z. Qiao, *Chem. Soc. Rev.* 43 (2014) 7787–7812.

[35] J.H. Yang, D.E. Wang, H.X. Han, C. Li, *Acc. Chem. Res.* 46 (2013) 1900–1909.

[36] F.Y. Wen, C. Li, *Acc. Chem. Res.* 46 (2013) 2355–2364.

[37] J. Bonde, P.G. Moses, T.F. Jaramillo, J.K. Norskov, I. Chorkendorff, *Faraday Discuss.* 140 (2009) 219–231.

[38] D. Merki, X. Hu, *Energy Environ. Sci.* 4 (2011) 3878–3888.

[39] I. Hatay, P. Ge, H. Vrubel, X. Hu, H.H. Girault, *Energy Environ. Sci.* 4 (2011) 4246–4251.

[40] E. Aslan, I.H. Patir, M. Ersöz, *ChemCatChem* 6 (2014) 2832–2835.

[41] F. Ozel, E. Aslan, A. Sarilmaz, I. HatayPatir, *ACS Appl. Mater. Interfaces* 8 (2016) 25881–25882.

[42] N. Li, M. Liu, Z. Zhou, J. Zhou, Y. Sun, L. Guo, *Nanoscale* 6 (2014) 9695–9702.

[43] D. Jing, M. Liu, Q. Chen, L. Guo, *Int. J. Hydrogen Energy* 35 (2010) 8521–8527.

[44] P.D. Tran, S.Y. Chiam, P.P. Boix, Y. Ren, S.S. Pramana, J. Fize, V. Artero, J. Barber, *Energy Environ. Sci.* 6 (2013) 2452–2459.

[45] P.D. Tran, M. Nguyen, S.S. Pramana, A. Bhattacharjee, S.Y. Chiam, J. Fize, M.J. Field, V. Artero, L.H. Wong, J. Loo, J. Barber, *Energy Environ. Sci.* 5 (2012) 8912–8916.

[46] A. Margalias, K. Seintis, M.Z. Yigit, M. Can, D. Sykridou, V. Giannetas, M. Fakis, E. Stathatos, *Dyes Pigments* 121 (2015) 316–327.

[47] C.J. Crossland, J.S. Evans, *Chem. Commun.* 18 (2003) 2292–2293.

[48] X. Hu, W. Shao, X. Hang, X. Zhang, W. Zhu, Y. Xie, *Angew. Chem. Int. Ed.* 55 (2016) 5733–5738.

[49] Z. Yu, F. Li, L. Sun, *Energy Environ. Sci.* 8 (2015) 760–775.

[50] W.J. Youngblood, S.H.A. Lee, Y. Kobayashi, E.A. Hernandez-Pagan, P. I. G. Hoertz, T.A. Moore, A.L. Moore, D. Gust, T.E. Mallouk, *J. Am. Chem. Soc.* 131 (2009) 926–927.

[51] Y. Park, W. Kim, D. Monllor-Satoca, T. Tachikawa, T. Majima, W. Choi, *J. Phys. Chem. Lett.* 4 (2013) 189–194.

[52] J. Zhao, Y. Ding, J. Wei, X. Du, Y. Yu, R. Han, *Int. J. Hydrogen Energy* 39 (2014) 18908–18918.

[53] J. Wang, K. Feng, H.-H. Zhang, B. Chen, Z.-J. Li, Q.-Y. Meng, L.-P. Zhang, C.-H. Tung, L.-Z. Wu, *Beilstein J. Nanotechnol.* 5 (2014) 1167–1174.

[54] M.K. Gonçalves, M. Dogru, E. Aslan, F. Ozel, I.H. Patir, M. Kus, M. Ersöz, *RSC Adv.* 5 (2015) 94025–94028.

[55] M.K. Gonçalves, E. Aslan, F. Ozel, I.H. Patir, *ChemSusChem* 9 (2016) 600–605.

[56] F. Ozel, E. Aslan, B. İstanbullu, O. Akay, I.H. Patir, *Appl. Catal. B: Environ.* 198 (2016) 67–73.

[57] R. Chauhan, M. Trivedi, L. Bahadur, Abhinav Kumar, *Chem. Asian J.* 6 (2011) 1525–1532.

[58] S.K. Choi, S. Kim, J. Ryu, S.K. Lim, H. Park, *Photochem. Photobiol. Sci.* 11 (2012) 1437–1444.